Research Paper

Intracranial self-stimulation reverses impaired spatial learning and regulates serum microRNA levels in a streptozotocin-induced rat model of Alzheimer disease

Andrea Riberas-Sánchez, MSc; Irene Puig-Parnau, PhD; Laia Vila-Solés, MSc; Soleil García-Brito, PhD; Laura Aldavert-Vera, PhD; Pilar Segura-Torres, PhD; Gemma Huguet, PhD; Elisabet Kádár, PhD

Background: The assessment of deep brain stimulation (DBS) as a therapeutic alternative for treating Alzheimer disease (AD) is ongoing. We aimed to determine the effects of intracranial self-stimulation at the medial forebrain bundle (MFB-ICSS) on spatial memory, neurodegeneration, and serum expression of microRNAs (miRNAs) in a rat model of sporadic AD created by injection of streptozotocin. We hypothesized that MFB-ICSS would reverse the behavioural effects of streptozotocin and modulate hippocampal neuronal density and serum levels of the miRNAs. **Methods:** We performed Morris water maze and light–dark transition tests. Levels of various proteins, specifically amyloid-β precurser protein (APP), phosphorylated tau protein (pTAU), and sirtuin 1 (SIRT1), and neurodegeneration were analyzed by Western blot and Nissl staining, respectively. Serum miRNA expression was measured by reverse transcription polymerase chain reaction. **Results:** Male rats that received streptozotocin had increased hippocampal levels of pTAU S202/T205, APP, and SIRT1 proteins; increased neurodegeneration in the CA1, dentate gyrus (DG), and dorsal tenia tecta; and worse performance in the Morris water maze task. No differences were observed in miRNAs, except for miR-181c and miR-let-7b. After MFB-ICSS, neuronal density in the CA1 and DG regions and levels of miR-181c in streptozotocin-treated and control rats were similar. Rats that received streptozotocin and underwent MFB-ICSS also showed lower levels of miR-let-7b and better spatial learning than rats that received streptozotocin without MFB-ICSS. **Limitations:** The reversal by MFB-ICSS of deficits induced by streptozotocin was fairly modest. **Conclusion:** Spatial memory performance, hippocampal neurodegeneration, and serum levels of miR-let-7b and miR-181c were affected by MFB-ICSS under AD-like conditions. Our results validate the MFB as a potential target for DBS and lend support to the use of specific miRNAs as promising biomarkers of the effectiveness of DBS in combatting AD-associated cognitive deficits.

Introduction

Alzheimer disease (AD), the most prevalent aging-related neurodegenerative disease, is characterized by progressive memory loss and cognitive dysfunction in older adults.[1] Although the underlying molecular mechanisms for AD are not fully understood, they have been reported to include various cellular events (synaptic damage, amyloid plaques, and neurofibrillary tangles, among others). These alterations are believed to progress from areas in the medial temporal lobe, such as the hippocampus, to other brain areas, such as the medial prefrontal cortex,[2] affecting the activity of different neural circuits.

Currently, the only 2 classes of drugs approved to treat AD symptoms do not cure or prevent the disease.[3] Deep brain stimulation (DBS) is currently being assessed as a potential therapeutic alternative to this pathologic circuitry condition in patients with AD. This neurosurgical procedure allows targeted, circuit-based neuromodulation using an intracranial electrode and a pulse generator.[4] The choice of DBS target is paramount in modulating the neural substrate that could reverse or slow the progression of AD. Unlike other brain targets of DBS, reinforcing stimulation of the medial forebrain bundle (MFB) simultaneously activates circuits related to the reinforcement itself and a wide variety of regions involved in several types of memory, such as the septum–hippocampal circuit, the amygdala, certain thalamic nuclei, and the prefrontal and retrosplenial cortices.[5] At the behavioural level, previous research has shown that intracranial self-stimulation at the MFB (MFB-ICSS) improves learning and memory in various tasks, in both young and

Correspondence to: E. Kádár, Street Maria Aurèlia Capmany 40, 17003, Girona, Spain, elisabet.kadar@udg.edu; G. Huguet, Street Maria Aurèlia Capmany 40, 17003, Girona, Spain, gemma.huguet@udg.edu; and S. Garcia-Brito, Street De la Fortuna s/n, 08193 Bellaterra, Barcelona, Spain, SoleilCristina.Garcia@uab.cat

Submitted May 4, 2023; Revised July 28, 2023; Revised Sept. 20, 2023; Revised Oct. 19, 2023; Accepted Oct. 19, 2023

Cite as: *J Psychiatry Neurosci* 2024 March 15;49(2). doi: 10.1503/jpn.230066

aged healthy rats,[6,7] as well as in patients with memory impairment caused by brain lesions.[8] Moreover, MFB-ICSS regulates the expression of proteins and specific microRNAs (miRNAs) related to synaptic plasticity.[9]

The miRNAs are a large family of small RNAs with an integral function in the regulation of gene expression. In the brain, miRNAs have been linked to neural plasticity events, and the dysregulation of their expression has been associated with several neurodegenerative conditions.[10] In addition, numerous studies have shown that their circulating levels are easily accessible, which thus allows their use as noninvasive biomarkers for AD diagnosis and prognosis.[11,12] However, there have been few conclusive studies regarding their usefulness in assessing the efficacy of therapeutic strategies.

Ninety-five percent of AD cases are not directly related to mutations in dominant genes, such as the genes for amyloid-β precursor protein (APP) or presenilin 1 and presenilin 2.[13] Thus, the use of a sporadic AD model, instead of a transgenic animal model, would be a valid approach to analyzing potential therapies. An increasing number of studies have shown that intracerebroventricular (ICV) injection of streptozotocin, a glucosamine–nitrosourea compound with diabetogenic action, triggers a sporadic AD-like pathology.[14–16]

In this study, we aimed to assess the effects of a post-training MFB-ICSS treatment on spatial learning and memory, neurodegeneration, and serum expression of 14 neural plasticity–related miRNAs in a rat model of sporadic AD created by ICV injection of streptozotocin. The first experiment was designed to confirm whether rats that received streptozotocin exhibited the main hallmarks of AD according to the references mentioned above. Once the model had been validated, the second experiment was designed to analyze the behavioural and molecular effects of MFB-ICSS on rats that received streptozotocin.

Methods

Animals

A total of 37 adult male Wistar rats (Harlan Laboratories; mean age 13.62 ± standard deviation [SD] 1.10 weeks and mean weight 395.74 ± SD 16.57 g at the time of surgery) were used for this study. The rats were individually housed in a controlled environment (21°C ± 1°C; humidity 60%; lights on from 0800 to 2000; food and water available ad libitum). All procedures were approved by the University Animal Welfare Committee, Universitat Autònoma de Barcelona (Ethics Committee on Animal and Human Experimentation, protocol number 4848 P1).

The timeline for the 2 experiments is shown in Figure 1. Experiment 1 aimed to validate the effects of streptozotocin on spatial memory, neurodegeneration, and hippocampal levels of the phosphorylated tau protein (pTAU), APP, and sirtuin 1 (SIRT1) proteins at 40 days after the infusion (n = 8 in control group; n = 7 in streptozotocin group). Experiment 2 assessed the effects of MFB-ICSS on spatial memory, neurodegeneration, and serum expression of candidate miRNAs in streptozotocin-infused rats (n = 6 in streptozotocin group; n = 9 in STZ+ICSS group; n = 7 in control group).

Intracerebroventricular injection of streptozotocin

Rats were anesthetized with a mixture of 5% isoflurane with oxygen, followed by 2.5% isoflurane to maintain anesthesia. With the animal set on a stereotactic apparatus, 2 small perforations were made to the skull, –0.7 mm anteroposterior (AP) and ±1.6 mm mediolateral (ML) from the bregma, according to a stereotaxic atlas.[17] For rats in the streptozotocin and STZ+ICSS groups, 8 µL of streptozotocin (2 mg/kg; Merck Life Science) was injected bilaterally ICV at

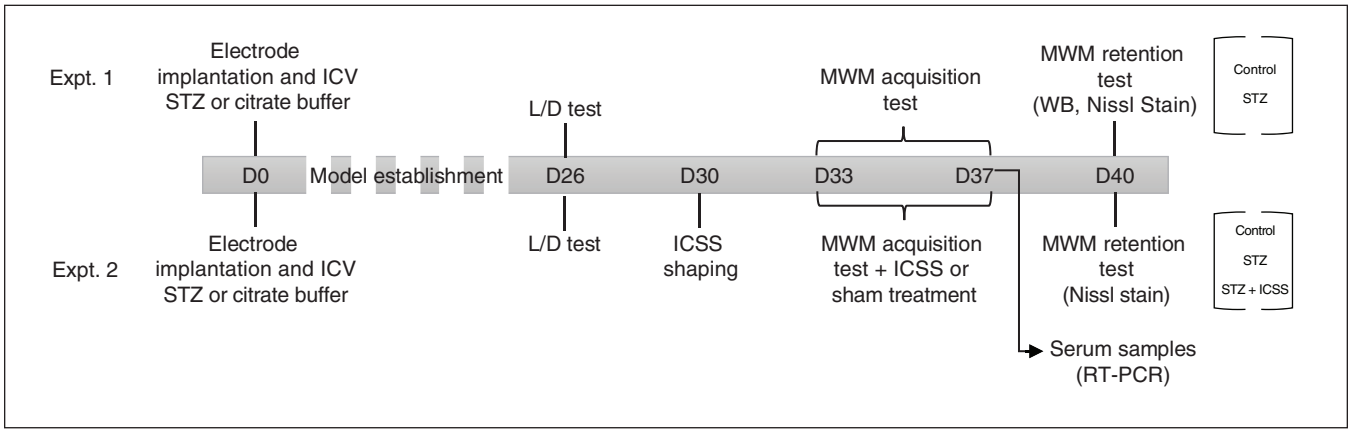

Figure 1: Timeline of the experimental design, using a schematic representation of experiments 1 and 2. On day 0 (D0) of each experiment, the rats underwent intracerebroventricular (ICV) infusion with streptozotocin (STZ) or vehicle (control), and a monopolar electrode was implanted and aimed at the midfrontal brain. A light–dark (L/D) transition test was carried out on day 26 (D26). Animals were trained on the Morris water maze (MWM) task between days 33 and 37 (D33 and D37, respectively) and were tested and euthanized on day 40 (D40) after injection. One group of STZ animals underwent 5 sessions of intracranial self-stimulation (ICSS) of the midfrontal brain after each MWM acquisition session (designated STZ+ICSS); animals in the STZ and control groups received sham treatment. RT-PCR = real-time polymerase chain reaction; WB = Western blot.

0.7 µL/min, –4.00 mm dorsoventral (DV) from the bregma, with the cranial surface as the dorsal reference. Rats in the control group received injections of vehicle (citrate buffer).

Long-term electrode implantation

After the ICV injection, a monopolar stainless steel electrode (diameter 150 µm) was implanted unilaterally in each rat, aimed at the MFB in the right lateral hypothalamus (–2.3 mm AP, –1.8 mm ML, –8.8 mm DV) (for details, see Vila-Solés and colleagues[18]). Appendix 1, Figure S1 (available at www.jpn.ca/lookup/doi/10.1503/jpn.230066/tab-related-content) depicts the exact location of the ICSS electrode tip for each rat in the STZ+ICSS group.

Light–dark transition test

Anxiety-like behaviour and exploratory behaviour in a novel environment were assessed using the light–dark transition test on day 26. The apparatus consisted of a box with a large bright compartment (310 × 310 × 240 mm) and a small dark compartment (200 × 310 × 240 mm), separated by a divider with an opening (100 × 100 mm). The test consisted of placing each rat in the bright compartment, facing away from the dark compartment, and allowing it to explore freely for a period of 5 minutes. The anxious response and exploratory behaviour were analyzed with variables such as latency to enter the dark compartment, number of transitions from one compartment to the other, number of head dips, number of rears, and percentage of time spent in each compartment.

Intracranial self-stimulation

On day 30, and before the spatial learning phase began, rats in the STZ+ICSS group were taught to self-stimulate by pressing a lever in a conventional Skinner box (24 × 27 × 30 cm; model LE850, Letica Scientific Instruments, Panlab). Electrical brain stimulation consisted of 0.3-second trains of 50-Hz sinusoidal waves (model CS2–10 stimulator, Cibertec). The ICSS behaviour of each animal was shaped to establish the range of current intensities generating responses on a continuous reinforcement schedule. Once a rat achieved a stable ICSS response rate (mean 82 responses/min), its optimal intensity was calculated as the average between the partial optimal intensities observed in the 2 sessions on days 30 and 31 (for details, see Vila-Solés and colleagues[18]). The optimal intensity was defined as the stimulation intensity at which a rat exhibited the maximum rate of lever presses. Each animal's optimal intensity was then used in its treatment sessions.

The ICSS treatment involved 5 sessions (1 session daily for 5 consecutive days, days 33 to 37), administered immediately after each acquisition session in the Morris water maze (MWM; described below). During each ICSS treatment session, the rat was placed in a self-stimulation box and was free to press the lever to self-administer 2500 trains of electrical stimulation at the pre-established optimal intensity, which ranged from 40 to 175 µA.

Rats receiving sham treatment (streptozotocin and control groups) were handled and placed in the Skinner box for 30 minutes but did not receive electrical stimulation.

Morris water maze

Spatial learning and memory were assessed using the MWM task. The characteristics of the apparatus and experimental conditions for this part of the study were described previously.[19] All animals had a single habituation session and a single 4-trial cued session on day 30, at 72 hours before the first acquisition session of spatial learning, to reduce emotional reactivity and to test the animals for their ability to swim to the cued goal.

For each rat, 5 MWM spatial acquisition sessions (designated A1, A2, A3, A4, and A5) were administered, once daily on days 33 to 37. Each session consisted of 2 trials, with a mean intertrial interval of 120 seconds. The retention or probe test was performed 72 hours after the last acquisition session (on day 40).

All swim paths were recorded using a closed-circuit video camera (Smart Video Tracking System, version 2.5, Panlab). The main outcome variable for the cued and spatial acquisition sessions were the latencies to target. In the probe test, the percentage of time spent in the target quadrant (TQ) in the first half of the trial (TQ30) and the entirety of the trial (TQ60), the percentage of time spent in the target annulus in each period (Ann30 and Ann60), and the average distance to target in each period (Dmt30 and Dmt60) were registered, where 30 and 60 refer to time in seconds. The percentage of time spent near the walls (within a distance of 15 cm; Walls30 and Walls60) and the speed (Speed30 and Speed60) across each trial and session, were analyzed as control variables for each group.

Sample collection

In experiment 1, the 2 hemispheres of each rat brain were collected separately, immediately after the probe test. From the left brain hemisphere (fixed in 4% formaldehyde in 0.01 mol/L phosphate-buffered saline for 24 hours at 4°C and cryopreserved in sucrose), serial coronal sections of 12 µm thickness were obtained in a cryostat (Reichert–Jung Cryocut 1800) at coordinates from –2.50 mm to –3.80 mm and from 2.00 mm to 3.50 mm AP to bregma to use for Nissl staining. From the right brain hemisphere, the dentate gyrus (DG) and the prelimbic cortex (PrL) were dissected as previously described by Puig-Parnau and colleagues[9] and stored in Allprotect tissue reagent (Qiagen) at –80°C until use.

In experiment 2, blood samples were collected from the lateral tail vein using capillary blood collection tubes (Microvette CB 300, Sarstedt S.A.U.), immediately after the last MFB-ICSS session. The tubes were maintained for 45 minutes at room temperature and centrifuged for 10 minutes at 3000 rpm to collect serum. After the probe test, the right hemisphere of each rat (ipsilateral to the electrode) was collected and processed to obtain histological sections for Nissl staining.

Total protein from DG or PrL sections and RNA from serum were extracted using the mirVana PARIS kit (Ambion). Tissue samples were first homogenized in cell disruption buffer, using a DIAX900 mechanical homogenizer (Heidolph). Serum samples (100 µL) were processed according to kit instructions. Lysed samples were centrifuged for 5 minutes at 18000*g* and 4°C for protein extraction. Protein quantification was performed using a Pierce BCA protein assay kit (Thermo Fisher Scientific) and a Synergy 4 spectrophotometer (BioTek).

Nissl staining

Slides were stained for 3 minutes with filtered 0.5% cresyl violet solution, rinsed in water for 5 minutes, and subsequently dehydrated and cover-slipped in Pertex medium. Photomicrographs for CA1, CA3, DG, PrL layers II and III, and dorsal tenia tecta (DTT) were obtained using a Vanox-T AH-2 microscope (Olympus). The number of neurons was counted manually, and neuronal density (a widely accepted metric for assessing neurodegeneration[20]) was measured in the various regions. In addition, in the PrL and DTT, where degenerating neurons could be easily identified as dark-stained neurons with shrunken cell bodies or presenting vacuolation, the percentage of cells with neurodegeneration was also quantified. Neuronal density and neurodegeneration were measured using Image J software, as shown in Appendix 1, Figure S2. The values for each animal were obtained by averaging the results for 3 sections.

Western blot

Total protein extracted from the DG and PrL were loaded onto Criterion TGX stain-free precast gels (Bio-Rad). Polyvinylidene fluoride membranes were incubated with the primary antibodies SIRT1 (07–131, Millipore; dilution 1:2000), APP (803001, Biolegend; dilution 1:2000), pTAU S202 and T205 (AT8 and MN1020, Thermo Fisher Scientific; dilution 1:1000), and pTAU S396 (AB109390, Abcam; dilution 1:70000) at 4ºC overnight and with total TAU (Tau46, sc-32274, Santa Cruz Biotechnology; dilution 1:2000) at room temperature for 1 hour, followed by incubation with peroxidase-conjugated secondary antibodies for 1 hour at room temperature and Immobilon Western Chemiluminescent HRP Substrate (EMD Millipore). Reactive bands were detected in a FluorChem luminometer and measured using FluorChem SP software (AlphaEaseFC). The relative intensities of the various proteins were normalized by comparing each band with the total protein lane, as described by Aldridge and colleagues.[21]

Quantitative real-time polymerase chain reaction for miRNA

Complementary DNA (cDNA) was synthesized and preamplified from 3 µL of serum RNA extract using the TaqMan Advanced miRNA cDNA synthesis kit in a Veriti 96-well thermal cycler (both from Applied Biosystems). Polymerase chain reactions (PCRs) were run on a QuantStudio 7, using the TaqMan Advanced miRNA quantitative PCR assay (Applied Biosystems). The relative quantity of each target miRNA was determined as $2^{-\Delta\Delta C_T}$ (where $\Delta\Delta C_T = \Delta Ct$ sample $- \Delta Ct$ reference sample; $\Delta Ct = Ct$ target $- Ct$ normalizer), using the mean of the control group as the reference sample and miR-let-7a-5p as the normalizer, these being the most stable endogenous candidates according to the NormFinder algorithm.[22]

Statistical analyses

The statistical analyses were performed using IBM SPSS Statistics 25 software. Analysis of performance in the MWM over several sessions or trials was conducted using mixed analysis of variance (ANOVA): in experiment 1, a 2 × 5 design; and in experiment 2, a 3 × 5 design (for group × session) for the acquisition phase of the spatial learning (average score of the 2 trials) and a 2 × 4 design (for group × trial) for the cued session.

Analysis of the retention test variables, the light–dark test results, and the molecular variables were assessed using the independent-sample *t* test or ANOVA, for parametric comparisons, or the Mann–Whitney *U* test or Kruskall–Wallis test, for nonparametric comparisons (according to the results of normality analysis), followed by the appropriate post hoc tests. In addition, a 1-sample *t* test against a constant was used for each group to determine whether the percentage of time spent in the TQ differed from chance (25%). Correlations between variables were estimated using the Spearman correlation test. Results were considered to be statistically significant when $p < 0.05$ with the 95% confidence interval.

Results

Behavioural, neurodegenerative, and molecular hippocampal alterations in rats that received streptozotocin

In terms of spatial learning in the MWM, the results of experiment 1 showed that both the control and streptozotocin groups acquired the task (session, $F_{4,52} = 2.876$, $p = 0.03$) as indicated by a decrease in latency, according to a similar significant downward linear function with some inflection (polynomial contrast; first grade, $p = 0.045$; fourth grade, $p = 0.03$). No relationship was observed between the exact location of the electrode and the behavioural outcome. However, the streptozotocin group showed worse performance (group, $F_{1,13} = 11.427$, $p = 0.005$) regardless of the session (group × session, $F_{4,52} = 0.654$, $p = 0.6$) (Figure 2A). Rats that received streptozotocin also showed deficient spatial retention 72 hours after the last acquisition session relative to the control group. The percentage of time in the TQ and the annulus was lower in the streptozotocin group during both the first 30 seconds (TQ30, $t_{13} = 2.228$, $p = 0.02$, $g = 1.085$; Ann30, $t_{13} = 2.509$, $p = 0.01$, $g = 1.222$) and the entire 60-second session (TQ60, $t_{13} = 1.959$, $p = 0.04$, $g = 0.954$; Ann60, $t_{13} = 2.078$, $p = 0.03$, $g = 1.012$) (Figure 2B). Additionally, only the control group performed above the level of chance (25%) in the TQ30 ($t_7 = 3.935$, $p = 0.006$) and TQ60 ($t_7 = 4.614$, $p = 0.002$) tests. Moreover, a trend toward

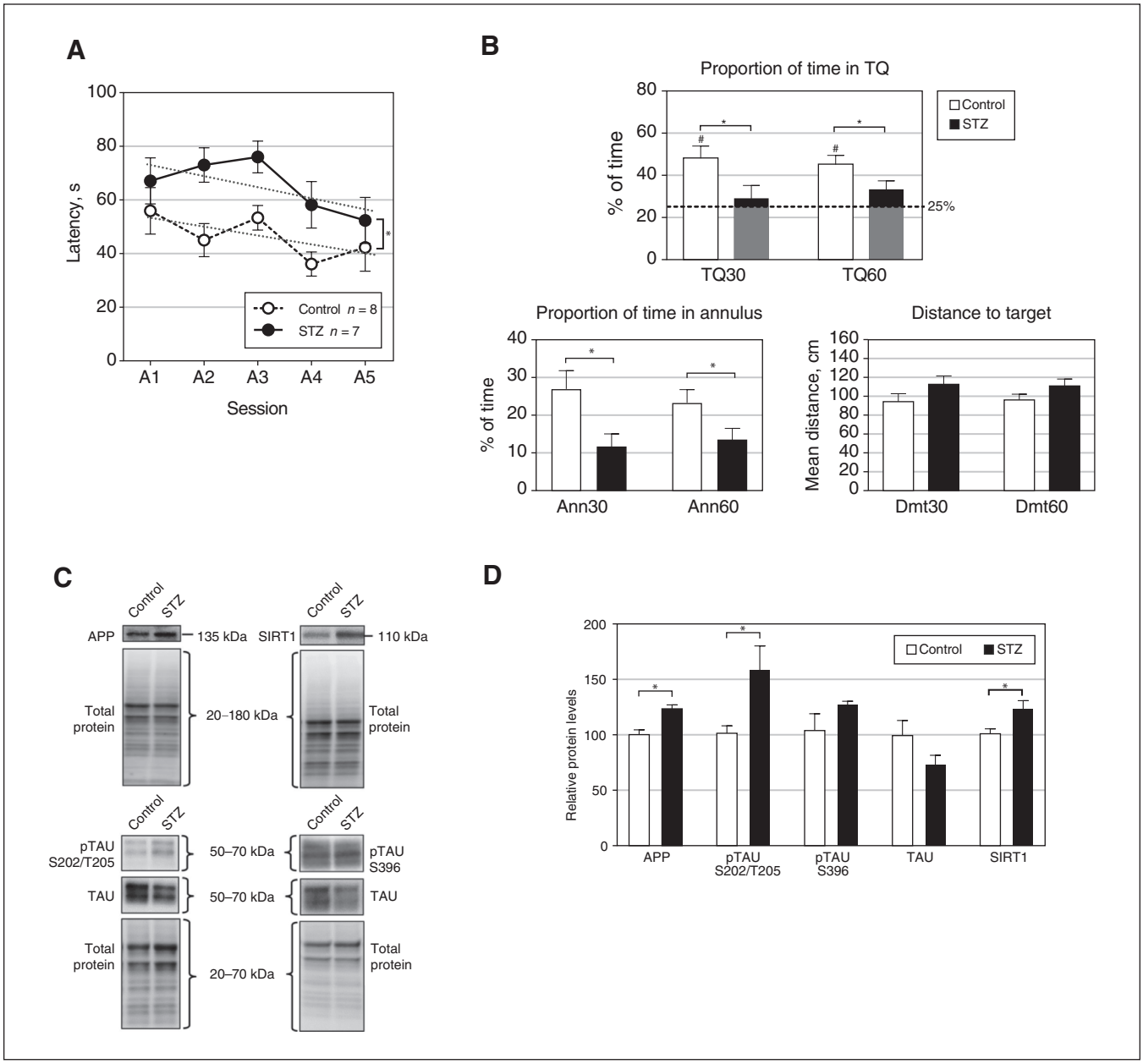

Figure 2: Effects of streptozotocin (STZ) on performance in the spatial Morris water maze test and protein levels in the dentate gyrus. (A) Escape latencies for the 5 acquisition sessions; linear trends for the control and STZ groups are represented by dotted lines. (B) Results in the retention test, at 30 and 60 seconds, respectively. TQ = percentage of time spent in the target quadrant; Ann = percentage of time spent in the annulus; Dmt = mean distance to target. The dashed line in the TQ graph represents chance (25%). (C) Representative Western blot results for amyloid-β precurser protein (APP), sirtuin 1 (SIRT1), phosphorylated tau protein (pTAU) S202/T205, pTAU S396, and tau protein (TAU), showing total protein band patterns in each case, for the control and STZ groups. (D) Levels of APP, pTAU S202/T205, pTAU S396, TAU, and SIRT1 proteins in the dentate gyrus for animals in the STZ and control groups. Throughout Figure 2, data represent mean ± standard error of the mean; #$p < 0.05$ relative to chance; *$p < 0.05$ for comparison between groups.

significantly larger Dmt30 and Dmt60 values was observed in the streptozotocin group relative to the control group ($t_{13} = 1.496$, $p = 0.08$, $g = 0.729$, and $t_{13} = 1.564$, $p = 0.07$, $g = 0.762$, respectively). No significant differences were observed between the groups in terms of time spent near the walls, in either the acquisition phase (group, $F_{1,13} = 2.416$, $p = 0.1$; group × session, $F_{4,52} = 1.157$, $p = 0.1$) (Appendix 1, Figure S3A) or the retention test (Walls30, $p = 0.3$; Walls60, $p = 0.2$) (Appendix 1, Figure S3B). In addition, there were no effects of streptozotocin on swimming speed in the retention test (Speed30, $p > 0.9$; Speed60, $p = 0.7$) (Appendix 1, Figure S3C).

In terms of the cued session, the rats that received streptozotocin eventually found the platform, guided by the discrete stimulus, with higher latencies than the control group (group, $F_{1,13} = 8.273$, $p = 0.01$) (Appendix 1, Figure S4A).

Relative levels of the following proteins in the DG were significantly higher in the streptozotocin group than the control group: APP ($t_{13} = 4.084$, $p = 0.001$, $g = 1.989$), pTAU S202/T205 ($t_{7.04} = 2.359$, $p = 0.05$, $g = 1.219$), and SIRT1 ($t_{13} = 2.506$, $p = 0.03$, $g = 1.220$) (Figure 2C and 2D). No differences in pTAU S396 were observed. In the control group, a significant positive correlation was found between pTAU S202/T205 and escape latency during session A1 ($\rho = 0.714$, $p = 0.047$), as well as between SIRT1 and session A2 latency ($\rho = 0.833$, $p = 0.01$). In streptozotocin-treated rats, there were positive correlations between pTAU and A2 latency ($\rho = 0.852$, $p = 0.02$), between SIRT1 and A5 latency ($\rho = 786$, $p = 0.04$), and between SIRT1 and Dmt60 ($\rho = 929$; $p = 0.003$) (Appendix 1, Table S1). No differences were observed in relative levels of any of the aforementioned proteins in the PrL (Appendix 1, Figure S5C and S5D).

Relative to control rats, the streptozotocin-treated rats showed a significant decrease in neuronal density in the CA1 ($t_{11} = 3.033$, $p = 0.006$, $g = 1.608$) and the DG ($t_{11} = 1.822$, $p = 0.048$, $g = 0.996$) (Figure 3A and 3B) but not in the CA3 (Appendix 1, Figure S6). No differences were found in the number of neurons in layers II and III of the PrL (Appendix 1, Figure S5A and S5B). In the DTT, no differences in neuronal density were detected ($t_{12} = 0.213$, $p = 0.4$, $g = 0.107$), but an increase in the percent neurodegeneration in the DTT was detected in streptozotocin-treated rats ($t_{12} = 3{,}123$ $p = 0.004$, $g = 1.562$) (Figure 3A and 3C).

Effects of MFB-ICSS on spatial learning and neurodegeneration in rats that received streptozotocin

In experiment 2, performance during the acquisition phase resulted in significant differences among the 3 experimental groups (group: $F_{2,19} = 7.142$, $p = 0.005$), regardless of the session (group × session: $F_{8,76} = 1.166$, $p = 0.3$). The streptozotocin group exhibited higher escape latencies compared with both the control group ($p = 0.001$) and the STZ+ICSS group ($p = 0.04$). No differences were observed between the STZ+ICSS and control groups (Figure 4A). The escape latencies for all groups followed linear functions (polynomial

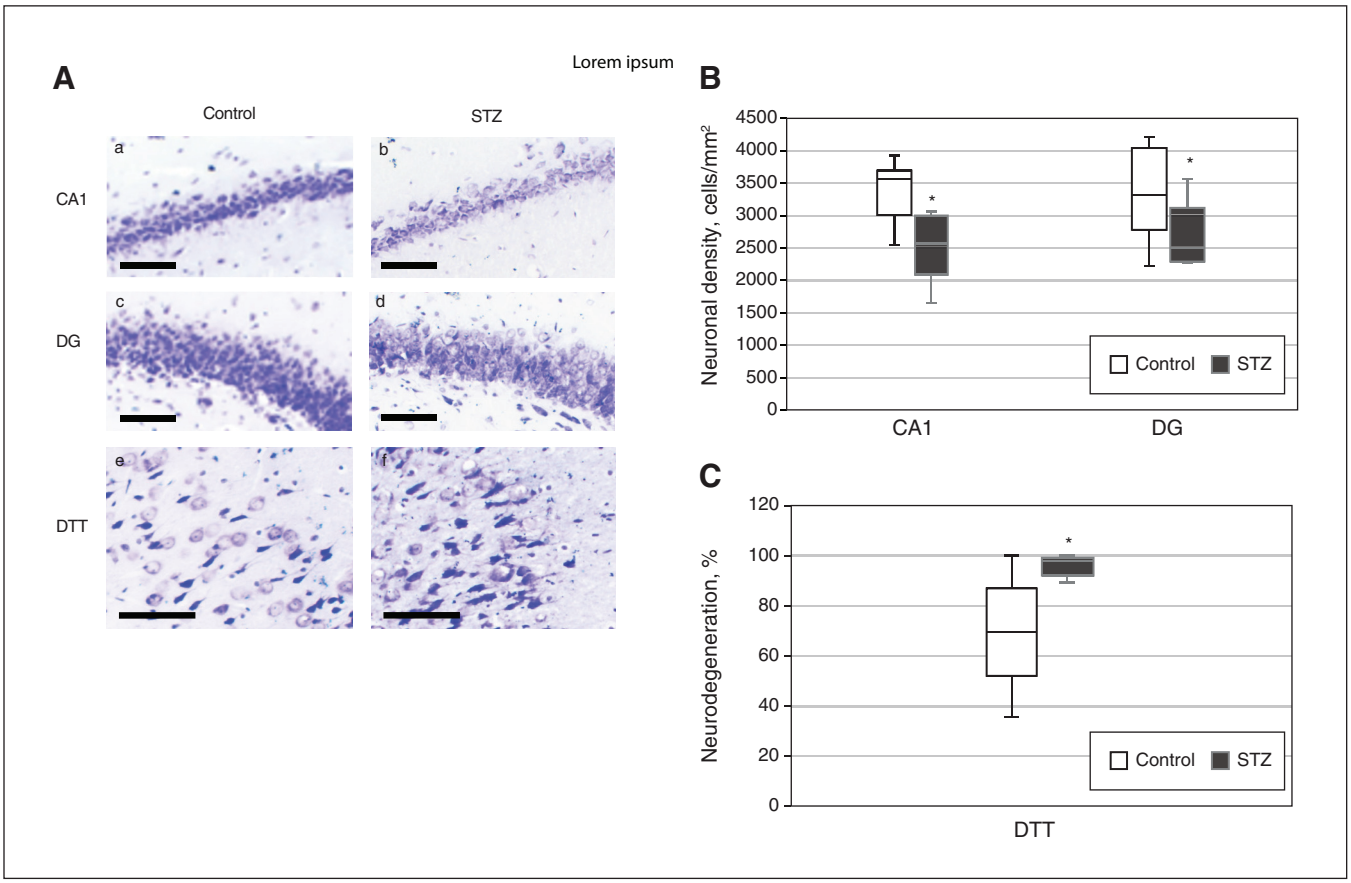

Figure 3: Effects of streptozotocin (STZ) on neurodegeneration in the CA1, dentate gyrus (DG), and dorsal tenia tecta (DTT) regions. (A) Representative photomicrographs of Nissl-stained sections of CA1 (a, b), DG (c, d), and DTT (e, f) for the control group (a, c, and e) and the STZ group (b, d, and f) (scale bar = 100 µm). (B) Neuronal density in the CA1 and DG regions, for the control and STZ groups. (C) Percent neurodegeneration in the DTT for the control and STZ groups. Data in Figure 3B and 3C represent mean ± standard error of the mean. *$p < 0.05$ relative to the control group.

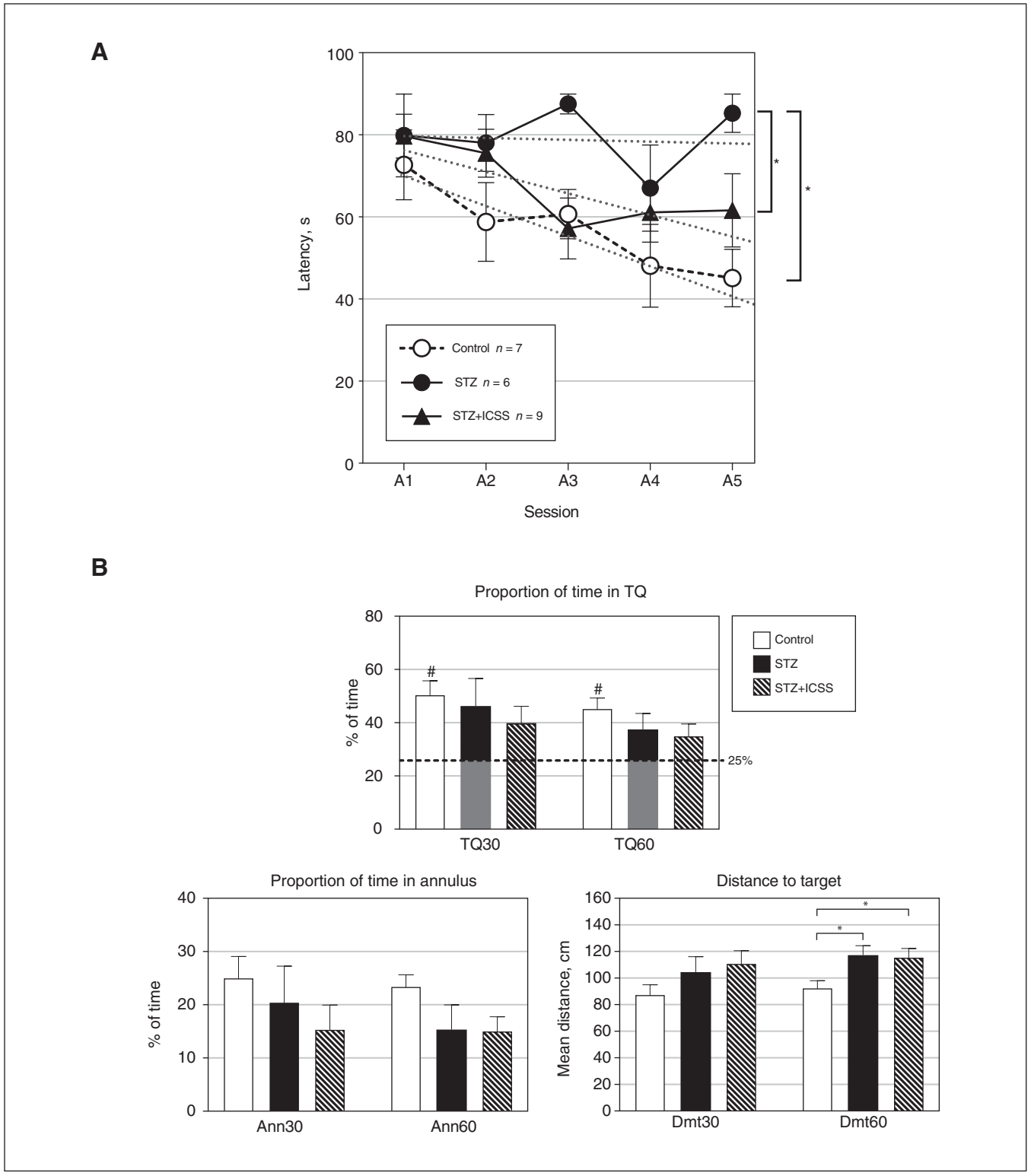

Figure 4: Effects of streptozotocin (STZ) and intracranial self-stimulation (ICSS) of the medial forebrain bundle on performance in the spatial Morris water maze (MWM) test. (A) Escape latencies for the 5 acquisition sessions in the MWM for control, STZ, and STZ+ICSS groups. Linear trends for each group are represented by dotted lines. (B) Results in the retention test, at 30 and 60 seconds, respectively. TQ = percentage of time spent in target quadrant; Ann = percentage of time spent in annulus; Dmt = mean distance to target. The dashed line in the TQ graph represents chance (25%). Throughout Figure 4, data represent mean ± standard error of the mean; #$p < 0.05$ relative to chance; *$p < 0.05$ for comparison between groups.

linear contrast; session, $F_{1,19} = 9.665$, $p = 0.006$; group × session, $F_{2,19} = 2.264$, $p = 0.1$). Examining simple effects within each group revealed a significant reduction in latencies between the first and the last acquisition sessions in the control ($p = 0.006$) and the STZ+ICSS ($p = 0.03$) groups, but not in the streptozotocin group.

Differences among experimental groups were also observed in the probe test for the Dmt60 variable ($F_{2,21} = 3.784$, $p = 0.04$, $\eta^2 = 0.285$). In this case, significantly worse performance was detected in both the streptozotocin and STZ+ICSS groups compared with the control group ($p = 0.02$ in both cases) (Figure 4B). Moreover, only the control group performed above the level of chance in TQ30 ($t_6 = 4.440$, $p = 0.004$) and TQ60 ($t_6 = 4.571$, $p = 0.004$).

In the acquisition phase, differences were observed between groups in the percentage of time spent near the walls ($F_{2,19} = 4.604$, $p = 0.02$), regardless of the session ($F_{8,76} = 1.406$, $p = 0.2$). The streptozotocin group spent more time near the walls than the other 2 groups (relative to control, $p = 0.008$; relative to STZ+ICSS, $p = 0.046$) (Appendix 1, Figure S3D). Differences between the streptozotocin group and the other groups were also observed for the Wall60 variable ($F_{2,21} = 4.865$, $p = 0.02$; control, $p = 0.007$; STZ+ICSS, $p = 0.03$) (Appendix 1, Figure S3E). In contrast, no significant differences among groups were observed with regard to Walls30 ($p = 0.3$) or swimming speed (Speed30, $p = 0.9$; Speed60, $p = 0.9$) (Appendix 1, Figure S3F).

During the cued session, differences were observed among groups (group, $F_{2,19} = 9.252$, $p = 0.002$). Latencies were similar between the streptozotocin-treated and STZ+ICSS groups, with both having higher latencies than the control animals (relative to streptozotocin, $p = 0.001$; relative to STZ+ICSS, $p = 0.006$) (Appendix 1, Figure S4B).

Additionally, there were no differences between the control and streptozotocin groups in the light–dark test carried out on day 26 (before the ICSS sessions in experiment 2), in either of the 2 experiments (Appendix 1, Figure S7).

In terms of effects on neurodegeneration, significant differences were observed among the 3 experimental groups in neuronal density of the CA1 and DG, as well as in the percent neurodegeneration in the DTT ($F_{2,18} = 6.899$, $p = 0.008$, $\eta^2 = 0.434$; $F_{2,18} = 2.852$, $p = 0.08$, $\eta^2 = 0.241$; and $F_{2,20} = 13.641$, $p = 0.001$, $\eta^2 = 0.577$, respectively). Replicating results from experiment 1, we found significant differences between the control and streptozotocin groups in terms of neuronal density of CA1 ($p = 0.002$) and DG ($p = 0.03$) and percent neurodegeneration in the DTT ($p = 0.008$). After the MFB-ICSS treatment, however, no differences in CA1 and DG neuronal densities were observed relative to the control group (Figure 5A and 5B). Percent neurodegeneration in the DTT remained significantly increased in the STZ+ICSS group compared with the control group ($p = 0.01$) (Figure 5C).

Circulating miRNAs regulated by MFB-ICSS in rats that received streptozotocin

In experiment 2, we analyzed the serum expression of 14 miRNAs related to neural plasticity and postulated them as potential biomarkers of AD. Of these, miR-134, miR-300, and miR-485 were below the limit of detection (< 32 Ct) in more than 85% of samples and therefore were not considered in further analyses. In addition, miR-154 was expressed in only 52% of all samples, with a frequency of 75%, 33%, and 55% in the control, streptozotocin, and STZ+ICSS groups, respectively, with no significant differences among them.

No significant differences were observed among the 3 experimental groups in levels of most of the other miRNAs that were analyzed (miR-16, miR-24, miR-132, miR-146a, miR-181a, miR-196a, miR-197, and miR-495); the only exceptions were miR-181c ($F_{2,16} = 6.720$, $p = 0.008$, $\eta^2 = 0.457$) and miR-let-7b ($H_2 = 6.738$, $p = 0.03$, $\varepsilon^2 = 0.034$). The rats that received streptozotocin had significantly lower serum levels of miR-181c than the control rats ($p = 0.007$). However, the STZ+ICSS rats displayed serum levels of miR-181c similar to those of control rats. Additionally, rats in the STZ+ICSS group exhibited significantly lower levels of miR-let-7b than those that received streptozotocin ($p = 0.02$) (Figure 6A).

The correlation analysis of serum miRNAs levels in the streptozotocin group revealed a significant negative correlation between miR-181c and miR-181a ($\rho = –0.886$, $p = 0.02$), as well as between miR-181a and neuronal densities in CA1 and CA3 ($\rho = –0.900$ $p = 0.04$, in both cases) (Appendix 1, Table S2). In STZ+ICSS rats, levels of miR-181c and miR-let-7b were negatively correlated with Dmt60 ($\rho = –0.786$, $p = 0.02$) and TQ60 ($\rho = –0.714$, $p = 0.047$) (Figure 6B).

Discussion

The use of animal models to reproduce a sporadic AD-like pathology is gaining popularity, because the most common forms of AD are also sporadic. Among the various animal models, ICV injection of a subdiabetogenic dose (1–3 mg/kg) of streptozotocin has been suggested as one of the most useful approaches to test therapeutic strategies.[23] In our laboratory, ICV injection of a 2 mg/kg dose led to establishment of a suitable model, whereas in a previous pilot experiment, a dose of 3 mg/kg resulted in high mortality. Our data are consistent with the findings of Moreira-Silva and colleagues,[24] indicating that 2 mg/kg is the optimal dose for modelling sporadic AD in Wistar rats. Furthermore, our results show that this dose also impairs rats' performance of a spatial learning task in the MWM, as previously reported in studies using higher doses.[25,26] Cued trials showed that the ability of streptozotocin-treated animals to learn to swim to a cued goal was also impaired. Thus, the injection of streptozotocin may have affected not only spatial learning but also other factors unrelated to place learning.[27] Given that streptozotocin did not affect swimming speed, exploratory behaviour in the light–dark transition test (rearing, transition, head dipping), or the rate of ICSS response, higher latency in cued and spatial learning did not seem to be a consequence of a sensory-motor alteration interfering with swimming toward the platform. In addition, the unaffected behaviour of the streptozotocin-treated rats in the light–dark test (latency, percentage of time in the light compartment) suggests that the observed effects of streptozotocin on learning tasks are

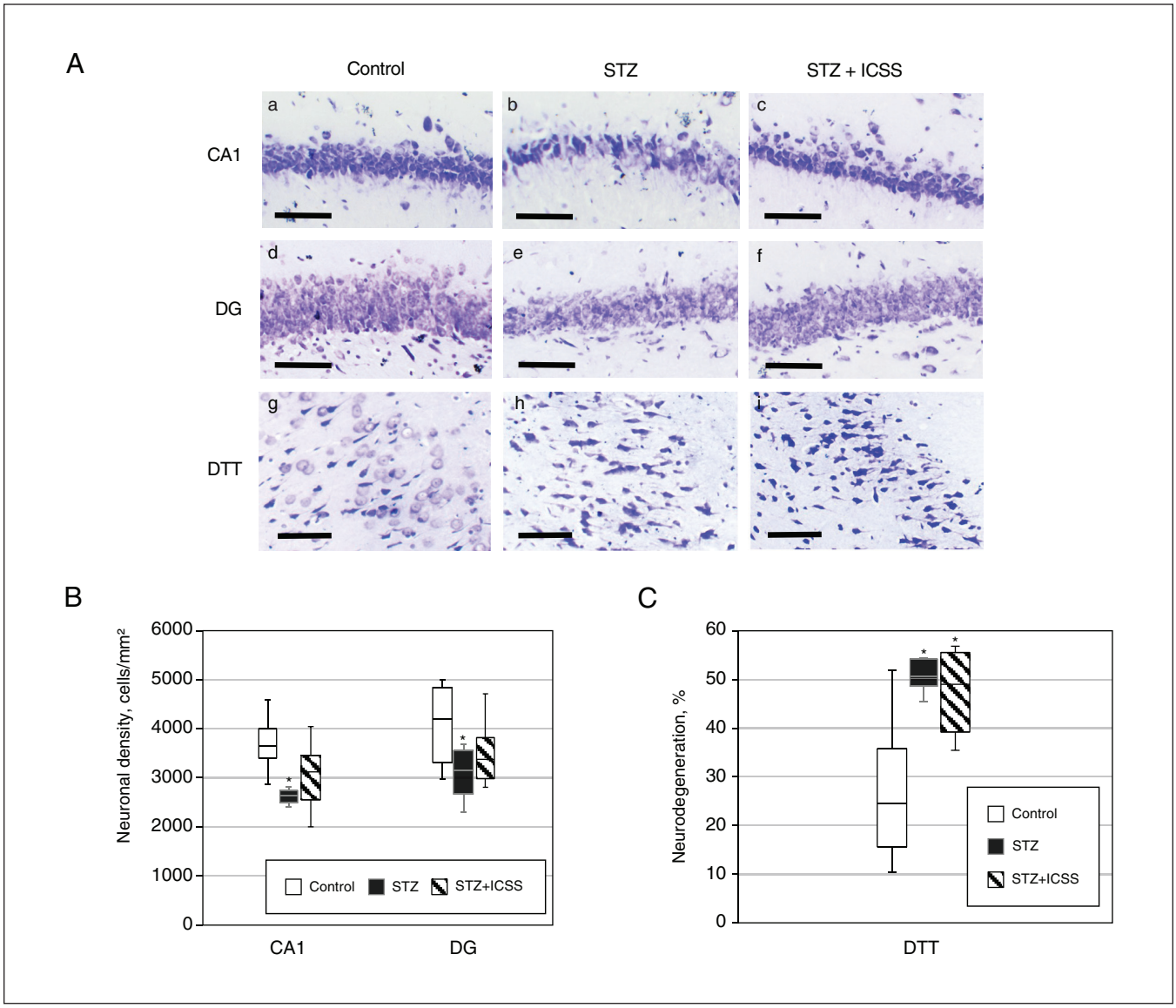

Figure 5: Effects of intracranial self-stimulation (ICSS) of the medial forebrain bundle on hippocampal neurodegeneration in rats treated with streptozotocin (STZ). (A) Representative photomicrographs of Nissl-stained sections of CA1 (a, b, c), dentate gyrus (DG) (d, e, f), and dorsal tenia tecta (DTT) (g, h, i) regions for control (a, d, and g), STZ (b, e, and h), and STZ+ICSS groups (c, f, and i) (scale bar = 100 μm). (B) Neuronal density in the CA1 and DG regions, for the control, STZ, and STZ+ICSS groups. (C) Percent neurodegeneration in the DTT region for the control, STZ, and STZ+ICSS groups. Data in Figure 5B and 5C represent mean ± standard error of the mean; *$p < 0.05$ relative to control.

unlikely to be primarily attributable to increased anxiety levels. Instead, the high thigmotactic behaviour observed in streptozotocin-treated rats may be interpreted as their inability to focus on the task. In any case, the fact that streptozotocin-treated rats eventually found the platform (with more training) implies that they possessed the necessary skills and motivation to accomplish the task. Overall, poor performance would indicate difficulty in achieving both associative and spatial learning, at least in this early stage of the AD model.

The streptozotocin dose of 2 mg/kg also induced neurodegeneration in the hippocampus at the cellular level. Our findings showed a significant decrease in neuronal density in the CA1 and DG, but not in layers II and III of the PrL, which are the layers most heavily involved in AD, according to Willumsen and colleagues.[28] Although most previous studies have focused on the hippocampus, reporting similar effects,[16,24,29,30] Esteves and colleagues[31] were the only ones to analyze the prelimbic region of the medial prefrontal cortex. In accordance with our findings, they reported no effects of streptozotocin on PrL cell density 3 months after ICV injection of the drug. The observed regional distribution of the histopathological effects in streptozotocin-treated rats, concentrated in the hippocampus and without prefrontal effects, could indicate that 37 days after ICV injection of

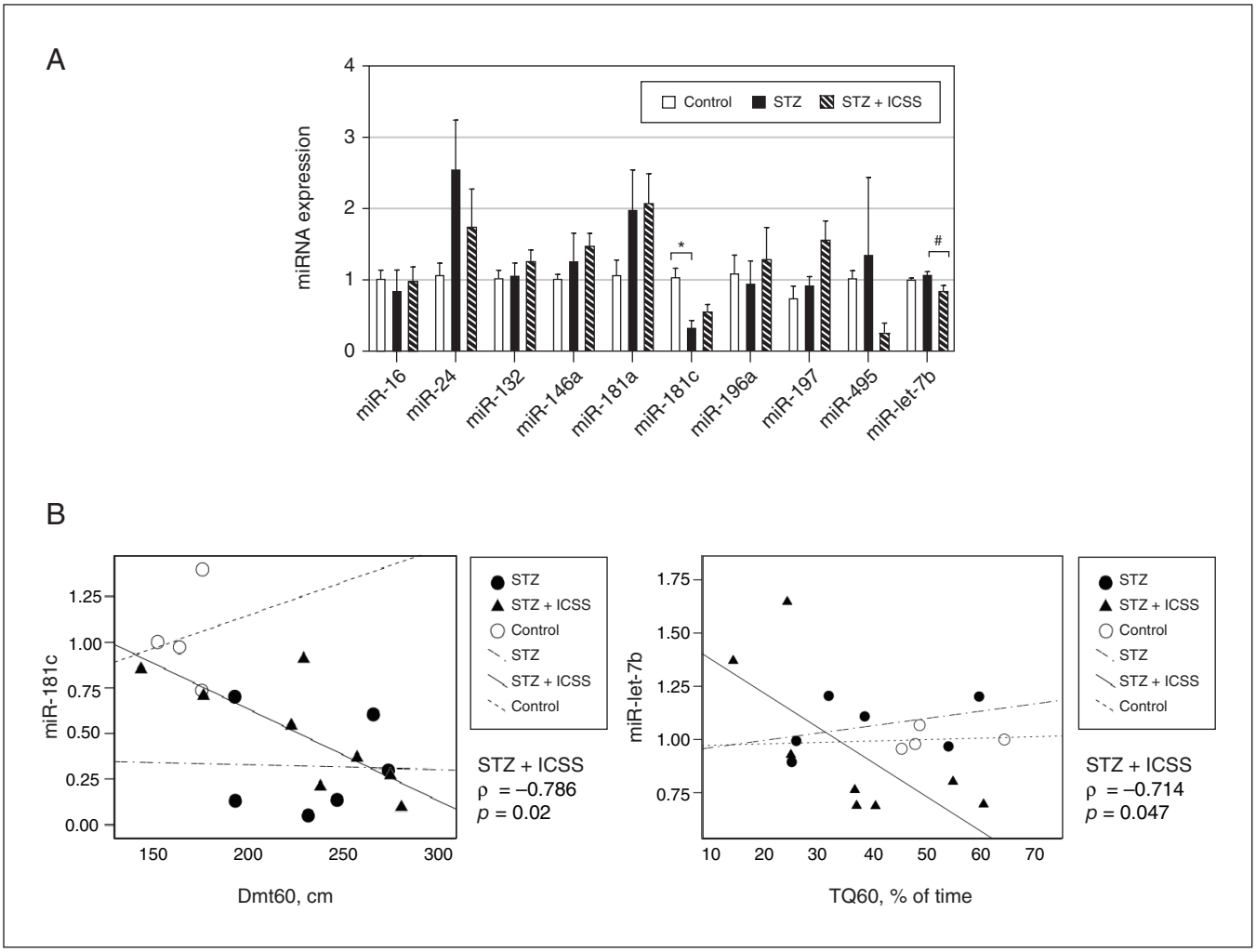

Figure 6: Effect of streptozotocin (STZ) and intracranial self-stimulation (ICSS) on serum micro-RNA (miRNA) levels and correlation with behavioural parameters. (A) Relative expression of miRNA candidates in control, STZ, and STZ+ICSS groups, calculated as $2^{-\Delta\Delta Ct}$, using let-7a-5p as the endogenous normalizer and the control group mean as the reference sample. Data represent mean ± standard error of the mean; *$p < 0.05$ relative to control; #$p < 0.05$ relative to STZ. (B) Correlation between miR-181c levels and distance to the target at 60 seconds (Dmt60) and between miR-let-7b levels and time in the target quadrant where the platform was located by 60 seconds (TQ60). Each dot represents a single rat in the control, STZ, or STZ+ICSS group, and the linear trend for each group is also shown.

streptozotocin represents an early stage of AD. Structural pathological changes would not have yet occurred in the PrL at this early stage, as has been described for human AD.[32] Our results are also in accordance with the stages of cognitive and structural change in the streptozotocin model described by Knezovic and colleagues.[33] To the best of our knowledge, our study is the first to detect neurodegeneration in the DTT following injection of streptozotocin. The DTT has recently been associated with robust odour-evoked activity, which suggests a prominent role in olfactory information processing, as well as in mediating communication between olfactory structures and the hippocampal formation.[34] These associations are especially interesting considering that olfactory deficits are detected in the early stages of AD.[35]

Our data, which show increased hippocampal levels of pTAU S202/T205 and APP but not pTAU S396 after injection of 2 mg/kg streptozotocin, are also in accordance with the findings of Moreira-Silva and colleagues[24] and confirm the dosage-dependent alteration of the S396 site reported by Zappa Villar and colleagues.[16] In addition, we observed a positive correlation between pTAU S202/T205 and escape latencies in the acquisition test. Interestingly, the presence and extent of pTAU-based neurofibrillary tangles pathology have been associated with disease duration and the severity of cognitive symptoms in AD.[36] Our results also showed a reduction in the total level of TAU in DG subfield extracts of streptozotocin-treated rats. Although a reduction in total TAU levels is not typically described as a feature of AD, time-dependent changes in expression levels of *Tau* have been reported following injection of streptozotocin. Thus, the reduction in total TAU levels could correspond to the biphasic pattern described in this model, whereby decreased *Tau*

expression levels are evident during the acute and subchronic response to streptozotocin.[37] Furthermore, our data showed an effect of streptozotocin on SIRT1 protein levels in the DG. Changes in *SIRT1* expression have been previously reported in a streptozotocin-induced (35–60 mg/kg) diabetic rat model[38] but not in a streptozotocin-induced AD model. The SIRT1 protein is a nicotinamide adenine dinucleotide (NAD^+)–dependent deacetylase associated with longevity and protection against aging-related neuronal degeneration and cognitive decline.[39] In contrast to studies showing reductions in SIRT1 levels in AD,[40,41] a significant increase in levels of this protein has also been observed in p25 transgenic AD mice[42] and patients with AD.[43] According to Elibol and Kilic,[43] the increase in SIRT1 levels could be a consequence of a compensatory mechanism against oxidative stress and decline in SIRT1 activity observed in older individuals and patients with AD. Thus, the increase in SIRT1 levels could result from decreased activity of SIRT1 in the streptozotocin-treated rats, which could explain why SIRT1 levels were positively correlated with worse behavioural performance. To further support this point, levels of SIRT1 recovered after withdrawal of amyloid-β peptides 1–42 have been linked to memory damage in hCMEC/D3 cells.[44]

Our findings suggest that MFB-ICSS treatment resulted in alleviation of the performance dysfunction of streptozotocin-treated rats on the spatial task, enabling them to achieve a performance level similar to that of the control group. These results are consistent with previous studies showing that MFB-ICSS compensates for severe cognitive impairment caused by lesions in brain regions involved in the evaluated tasks.[8,42] This phenomenon could be related to the fact that such treatment can activate plasticity mechanisms in multiple brain memory systems,[45–50] possibly explaining its effectiveness. However, unlike our previous AD model, which involved amyloid-β administration,[51] the MFB-ICSS treatment was unable to reverse retention impairment at 72 hours. This could be explained by the different degrees of disruption caused by streptozotocin and amyloid-β at various points of the learning and memory task. Whereas animals that received streptozotocin injections showed substantial impairment in the first MWM acquisition, the amyloid-β infusion exclusively affected task retention. It is possible that a greater number of stimulation sessions are required to maintain the effects on memory consolidation.

Our results also suggest that MFB-ICSS could reverse the decrease in neuronal density observed in the CA1 and DG, but the analysis suggested only a partial improvement in neurodegeneration, given that differences were detected only in the comparison of MFB-ICSS and control rats. However, the DTT area did not show any sign of reversal. This finding could suggest a lack of effect of MFB-ICSS in this olfactory-related area or could indicate that the rats had reached a neurodegenerative stage that was difficult to reverse.

Taken together, and although the MFB-ICSS reversal of spatial learning deficits induced by streptozotocin was fairly modest, our results support the potential of MFB stimulation for treating AD-affected circuitry. The partial reversal of deficits may be due to high intersubject variability after treatment. However, we previously reported that MFB-ICSS improved memory impairments and reduced pathological hallmarks in a rat model of AD with amyloid-β infusion.[51] Nonetheless, it remains unknown whether the response to stimulation is stable over time in both cases. Some clinical trials have pointed out that the DBS effect in AD is only temporary,[52] whereas recent studies on tremor syndromes have suggested that alternating DBS (once a week for 12 weeks) produces better results than stimulation with constant parameters.[53,54] Further longitudinal follow-up studies in animal models of AD, with comparison of different stimulation programs, are required to validate the beneficial effects of DBS and guide its future clinical applications.

To the best of our knowledge, this study is the first to analyze the effects of DBS treatment on the serum expression of a subset of neural plasticity–related miRNAs in a model of sporadic AD. Of the miRNAs considered, miR-16, miR-24, miR-132, miR-146a, miR-181a, miR-196a, miR-197, and miR-495 did not show any significant differences in the streptozotocin or STZ+ICSS groups relative to the control group. Only miR-181c and miR- let-7b were differentially expressed after treatment with streptozotocin and MFB-ICSS. In addition, miR-181c has been reported to be consistently downregulated in the blood and cortex of patients with AD.[55] Its loss of function in primary cortical neurons results in reduced synaptogenesis,[56] whereas its upregulation has been linked to learning and memory.[57] Here, serum levels of miR-181c were lower in streptozotocin-treated rats than in control rats, with no significant alteration observed when rats in the STZ+ICSS group were compared with control rats. Considering the studies that have shown associations between serum and tissue miRNA levels[58,59] and based on our previous findings showing upregulation of hippocampal miR-181c levels by MFB-ICSS in healthy rats,[9] we hypothesize that MFB-ICSS can reverse the memory and learning deficits in streptozotocin-treated rats by modulating levels of hippocampal miR-181c. To examine this hypothesis, further research should aim to induce inhibition of miR-181c in the hippocampus of rats with AD-like pathology and analyze the effects of MFB-ICSS on behaviour and on the expression of its putative targets.

We also found that miR-181c was negatively correlated with another member of the miR-181 family,[60] miR-181a. Previous studies have reported miR-181a upregulation in blood samples of patients with AD[61] and an association with decreased SIRT1 expression.[62] Consistent with the idea that miR-181a is involved in the progression of AD,[61] our study shows that serum levels of this miRNA were negatively associated with hippocampal neuronal density in rats that received streptozotocin, whereas this association was positive for miR-181c.

We also found lower miR-let-7b levels in rats that underwent MFB-ICSS compared with those that received streptozotocin. Cerebrospinal fluid from patients with AD has been shown to contain higher amounts of miR-let-7b compared with healthy controls,[63] and its levels have been associated with increased severity of AD.[64] Our results also showed a significant association between levels of miR-181c and miR-let-7b and performance on the retention test, whereby

rats with lower levels of miR-181c and higher levels of miR-let-7b had worse performance.

Our results indicate that the streptozotocin model may mimic the alteration of certain miRNAs that have been found in the serum of patients with AD. In addition, it appears that MFB-ICSS could modulate the serum levels of miR-181c and miR-let-7-b in opposite directions. Given the key role of these miRNAs in the pathogenesis of AD, further studies analyzing their potential as biomarkers of treatment effects would be of great biomedical relevance.

Conclusion

This study confirmed that bilateral ICV injection of streptozotocin (2 mg/kg) can be used to reproduce certain distinctive neuropathologic features of AD, including neurodegeneration and hippocampal overexpression of pTAU S202/T205 and APP, as well as deficits in a spatial memory task at 40 days after the injection. Administration of this dose of streptozotocin also induced a substantial increase in SIRT1 and a reduction in serum levels of miR-181c, both of which are detected in patients with AD, highlighting the potential of this animal model as a realistic model of sporadic AD. Furthermore, our results indicate that post-training MFB-ICSS treatment rescues deficits in a spatial learning task and miR-let-7b serum levels while partially reversing changes in CA1 neuronal density and miR-181c serum levels. Serum levels of both miRNAs were correlated with MWM performance of MFB-ICSS–treated rats that received streptozotocin. As such, miR-181c and miR-let-7-b may serve as potential biomarkers for assessing the effectiveness of DBS in combatting cognitive deficits in AD.

Acknowledgements: The authors thank Carlos Baldellou Estrada and Cristina Gerboles Freixas for their technical contributions.

Affiliations: From the Department of Biology, Faculty of Science, Universitat de Girona, Girona, Spain (Riberas-Sánchez, Puig-Parnau, Huguet, Kádár); and the Psychobiology Unit, Institute of Neurosciences, Universitat Autònoma de Barcelona, Bellaterra, Barcelona, Spain (Vila-Solés, García-Brito, Aldavert-Vera, Segura-Torres).

Competing interests: None declared.

Contributors: Laura Aldavert-Vera, Pilar Segura-Torres, and Gemma Huguet were responsible for conception and design of the study. Andrea Riberas-Sánchez, Irene Puig-Parnau, Laia Vila-Solés, and Soleil García-Brito acquired the data, and Elisabet Kádár analyzed and interpreted the data. Andrea Riberas-Sánchez, Irene Puig-Parnau, Laia Vila-Solés, Soleil García-Brito, Laura Aldavert-Vera, Gemma Huguet, and Elisabet Kádár contributed to writing the manuscript, and Pilar Segura-Torres critically reviewed the manuscript for important intellectual content. All of the authors approved the final version for publication and agreed to be accountable for the work.

Funding: This work was supported by grants PID2020-117101RB-C21 and PDI2020-117101RB-C22 from the Ministerio de Ciencia e Innovación, Spain. Andrea Riberas-Sánchez received a predoctoral fellowship from the Universitat de Girona (IFUdG2022/63).

References

1. Khan S, Barve KH, Kumar MS. Recent advancements in pathogenesis, diagnostics and treatment of Alzheimer's disease. *Curr Neuropharmacol* 2020;18:1106-25.
2. Rüb U, Stratmann K, Heinsen H, et al. The brainstem tau cytoskeletal pathology of Alzheimer's disease: a brief historical overview and description of its anatomical distribution pattern, evolutional features, pathogenic and clinical relevance. *Curr Alzheimer Res* 2016;13:1178-97.
3. Breijyeh Z, Karaman R. Comprehensive review on Alzheimer's disease: causes and treatment. *Molecules* 2020;25:5789.
4. Krauss JK, Lipsman N, Aziz T, et al. Technology of deep brain stimulation: current status and future directions. *Nat Rev Neurol* 2021;17:75-87.
5. Morgado-Bernal I, Segura-Torres P. Intracranial self-stimulation and memory in rats: a sistematic review. *Psicothema* 2022;34:446-53.
6. Redolar-Ripoll D, Soriano Mas C, Guillazo Blanch G, et al. Post-training intracranial self-stimulation ameliorates the detrimental effects of parafascicular thalamic lesions on active avoidance in young and aged rats. *Behav Neurosci* 2003;117:246-56.
7. Aldavert-Vera L, Costa-Miserachs D, Massanés-Rotger E, et al. Facilitation of a distributed shuttle-box conditioning with post-training intracranial self-stimulation in old rats. *Neurobiol Learn Mem* 1997;67:254-8.
8. Kádár E, Ramoneda M, Aldavert-Vera L, et al. Rewarding brain stimulation reverses the disruptive effect of amygdala damage on emotional learning. *Behav Brain Res* 2014;274:43-52.
9. Puig-Parnau I, Garcia-Brito S, Faghihi N, et al. Intracranial self-stimulation modulates levels of SIRT1 protein and neural plasticity-related microRNAs. *Mol Neurobiol* 2020;57:2551-62.
10. Kuss AW, Chen W. MicroRNAs in brain function and disease. *Curr Neurol Neurosci Rep* 2008;8:190-7.
11. Silvestro S, Bramanti P, Mazzon E. Role of miRNAs in Alzheimer's disease and possible fields of application. *Int J Mol Sci* 2019;20:3979.
12. Klyucherev TO, Olszewski P, Shalimova AA, et al. Advances in the development of new biomarkers for Alzheimer's disease. *Transl Neurodegener* 2022;11:25.
13. Drummond E, Wisniewski T. Alzheimer's disease: experimental models and reality. *Acta Neuropathol* 2017;29:155-75.
14. Mishra SK, Singh S, Shukla S, et al. Intracerebroventricular streptozotocin impairs adult neurogenesis and cognitive functions via regulating neuroinflammation and insulin signaling in adult rats. *Neurochem Int* 2018;113:56-68.
15. Voronkov DN, Stavrovskaya AV, Stelmashook EV, et al. Neurodegenerative changes in rat brain in streptozotocin model of Alzheimer's disease. *Bull Exp Biol Med* 2019;166:793-6.
16. Zappa Villar MF, Hanotte JL, Lockhart EF, et al. Intracerebroventricular streptozotocin induces impaired Barnes maze spatial memory and reduces astrocyte branching in the CA1 and CA3 hippocampal regions. *J Neural Transm (Vienna)* 2018;125:1787-803.
17. Paxinos G, Watson C. *The rat brain in sterotaxic coordinates.* Cambridge (MA): Academic Press; 2016.
18. Vila-Solés L, García-Brito S, Aldavert-Vera L, et al. Protocol to assess rewarding brain stimulation as a learning and memory modulating treatment: comparison between self-administration and experimenter-administration. *Front Behav Neurosci* 2022;16:1046259.
19. García-Brito S, Aldavert-Vera L, Huguet G, et al. Orexin-1 receptor blockade differentially affects spatial and visual discrimination memory facilitation by intracranial self-stimulation. *Neurobiol Learn Mem* 2020;169:107188.
20. Fronza MG, Baldinotti R, Sacramento M, et al. Effect of QTC-4-MeOBnE treatment on memory, neurodegeneration, and neurogenesis in a streptozotocin-induced mouse model of Alzheimer's disease. *ACS Chem Neurosci* 2021;12:109-22.
21. Aldridge GM, Podrebarac DM, Greenough WT, et al. The use of total protein stains as loading controls: an alternative to high-abundance single protein controls in semi-quantitative immunoblotting. *J Neurosci Methods* 2008;172:250-4.

22. Andersen CL, Jensen JL, Ørntoft TF. Normalization of real-time quantitative reverse transcription-PCR data: a model-based variance estimation approach to identify genes suited for normalization, applied to bladder and colon cancer data sets. *Cancer Res* 2004;64:5245-50.
23. Salkovic-Petrisic M, Knezovic A, Hoyer S, et al. What have we learned from the streptozotocin-induced animal model of sporadic Alzheimer's disease, about the therapeutic strategies in Alzheimer's research? *J Neural Transm (Vienna)* 2013;120:233-52.
24. Moreira-Silva D, Vizin RCL, Martins TMS, et al. Intracerebral injection of streptozotocin to model Alzheimer disease in rats. *Bio Protoc* 2019;9:e3397.
25. Pilipenko V, Narbute K, Amara I, et al. GABA-containing compound gamma pyrone protects against brain impairments in Alzheimer's disease model male rats and prevents mitochondrial dysfunction in cell culture. *J Neurosci Res* 2019;97:708-26.
26. Zafeer MF, Firdaus F, Anis E, et al. Prolong treatment with transferulic acid mitigates bioenergetics loss and restores mitochondrial dynamics in streptozotocin-induced sporadic dementia of Alzheimer's type. *Neurotoxicology* 2019;73:246-57.
27. Vorhees CV, Williams MT. Morris water maze: procedures for assessing spatial and related forms of learning and memory. *Nat Protoc* 2006;1:848-58.
28. Willumsen N, Poole T, Nicholas JM, et al. Variability in the type and layer distribution of cortical Aβ pathology in familial Alzheimer's disease. *Brain Pathol* 2022;32:e13009.
29. de la Monte SM, Tong M, Schiano I, et al. Improved brain insulin/IGF signaling and reduced neuro inflammation with T3D-959 in an experimental model of sporadic Alzheimer's disease. *J Alzheimers Dis* 2017;55:849-64.
30. Hashemi-Firouzi N, Shahidi S, Soleimani-Asl S, et al. 5-Hydroxytryptamine receptor 6 antagonist, SB258585 exerts neuroprotection in a rat model of streptozotocin-induced Alzheimer's disease. *Metab Brain Dis* 2018;33:1243-53.
31. Esteves IM, Lopes-Aguiar C, Rossignoli MT, et al. Chronic nicotine attenuates behavioral and synaptic plasticity impairments in a streptozotocin model of Alzheimer's disease. *Neuroscience* 2017;353:87-97.
32. Braak H, Alafuzoff I, Arzberger T, et al. Staging of Alzheimer disease-associated neurofibrillary pathology using paraffin sections and immunocytochemistry. *Acta Neuropathol* 2006;112:389-404.
33. Knezovic A, Osmanovic-Barilar J, Curlin M, et al. Staging of cognitive deficits and neuropathological and ultrastructural changes in streptozotocin-induced rat model of Alzheimer's disease. *J Neural Transm (Vienna)* 2015;122:577-92.
34. Cousens GA. Characterization of odor-evoked neural activity in the olfactory peduncle. *IBRO Rep* 2020;9:157-63.
35. Murphy C. Olfactory and other sensory impairments in Alzheimer disease. *Nat Rev Neurol* 2019;15:11-24.
36. Chandra A, Valkimadi PE, Pagano G, et al. Applications of amyloid, tau, and neuroinflammation PET imaging to Alzheimer's disease and mild cognitive impairment. *Hum Brain Mapp* 2019;40:5424-42.
37. Barilar JO, Knezovic A, Grünblatt E, et al. Nine-month follow-up of the insulin receptor signalling cascade in the brain of streptozotocin rat model of sporadic Alzheimer's disease. *J Neural Transm (Vienna)* 2015;122:565-76.
38. Abo El-Nasr NME, Saleh DO, Hashad IM. Role of olmesartan in ameliorating diabetic nephropathy in rats by targeting the AGE/PKC, TLR4/P38-MAPK and SIRT-1 autophagic signaling pathways. *Eur J Pharmacol* 2022;928:175117.
39. Pukhalskaia AE, Dyatlova AS, Linkova NS, et al. Sirtuins as possible predictors of aging and Alzheimer's disease development: verification in the hippocampus and saliva. *Bull Exp Biol Med* 2020;169:821-4.
40. Julien C, Tremblay C, Émond V, et al. SIRT1 decrease parallels the accumulation of tau in Alzheimer disease. *J Neuropathol Exp Neurol* 2009;68:48-58.
41. Lutz MI, Milenkovic I, Regelsberger G, et al. Distinct patterns of sirtuin expression during progression of Alzheimer's disease. *Neuromolecular Med* 2014;16:405-14.
42. Kim D, Nguyen MD, Dobbin MM, et al. SIRT1 deacetylase protects against neurodegeneration in models for Alzheimer's disease and amyotrophic lateral sclerosis. *EMBO J* 2007;26:3169-79.
43. Elibol B, Kilic U. High levels of SIRT1 expression as a protective mechanism against disease-related conditions. *Front Endocrinol (Lausanne)* 2018;9:614.
44. Liu H, Zhang Y, Zhang H, et al. Aβ-Induced damage memory in hCMEC/D3 cells mediated by sirtuin-1. *Int J Mol Sci* 2020;21:8226.
45. Segura-Torres P, Aldavert-Vera L, Gatell-Segura A, et al. Intracranial self-stimulation recovers learning and memory capacity in basolateral amygdala-damaged rats. *Neurobiol Learn Mem* 2010;93:117-26.
46. Aldavert-Vera L, Huguet G, Costa-Miserachs D, et al. Intracranial self-stimulation facilitates active-avoidance retention and induces expression of c-Fos and Nurr1 in rat brain memory systems. *Behav Brain Res* 2013;250:46-57.
47. Arvanitogiannis A, Tzschentke TM, Riscaldino L, et al. Fos expression following self-stimulation of the medial prefrontal cortex. *Behav Brain Res* 2000;107:123.
48 Huguet G, Aldavert-Vera L, Kádár E, et al. Intracranial self-stimulation to the lateral hypothalamus, a memory improving treatment, results in hippocampal changes in gene expression. *Neuroscience* 2009;162:359-74.
49. Kadar E, Aldavert-Vera L, Huguet G, et al. Intracranial self-stimulation induces expression of learning and memory-related genes in rat amygdala. *Genes Brain Behav* 2011;10:69-77.
50. Kádár E, Vico-Varela E, Aldavert-Vera L, et al. Increase in c-Fos and Arc protein in retrosplenial cortex after memory-improving lateral hypothalamic electrical stimulation treatment. *Neurobiol Learn Mem* 2016;128:117-24.
51. Puig-Parnau I, Garcia-Brito S, Vila-Soles L, et al. Intracranial self-stimulation of the medial forebrain bundle ameliorates memory disturbances and pathological hallmarks in an Alzheimer's disease model by intracerebral administration of amyloid-β in rats. *Neuroscience* 2023;512:16-31.
52. Lozano AM, Fosdick L, Chakravarty MM, et al. A phase II study of fornix deep brain stimulation in mild Alzheimer's disease. *J Alzheimers Dis* 2016;54:777-87.
53. Seier M, Hiller A, Quinn J, et al. Alternating thalamic deep brain stimulation for essential tremor: a trial to reduce habituation. *Mov Disord Clin Pract (Hoboken)* 2018;5:620-6.
54. Peters J, Tisch S. Habituation after deep brain stimulation in tremor syndromes: prevalence, risk factors and long-term outcomes. *Front Neurol* 2021;12:696950.
55. Sun C, Liu J, Duan F, et al. The role of the microRNA regulatory network in Alzheimer's disease: a bioinformatics analysis. *Arch Med Sci* 2021;18:206-22.
56. Kos A, Olde Loohuis N, Meinhardt J, et al. MicroRNA-181 promotes synaptogenesis and attenuates axonal outgrowth in cortical neurons. *Cell Mol Life Sci* 2016;73:3555-67.
57. Fang C, Li Q, Min G, et al. MicroRNA-181c ameliorates cognitive impairment induced by chronic cerebral hypoperfusion in rats. *Mol Neurobiol* 2017;54:8370-85.
58. Weiland M, Gao XH, Mi QS. Small RNAs have a large impact: circulating microRNAs as biomarkers for human diseases. *RNA Biol* 2012;9:850-9.
59. Voelz C, Ebrahimy N, Zhao W, et al. Transient focal cerebral ischemia leads to miRNA alterations in different brain regions, blood serum, liver and spleen. *Int J Mol Sci* 2021;23:161.
60. Indrieri A, Carrella S, Carotenuto P, et al. The pervasive role of the miR-181 family in development, neurodegeneration, and cancer. *Int J Mol Sci* 2020;21:2092.
61. Ansari A, Maffioletti E, Milanesi E, et al. miR-146a and miR-181a are involved in the progression of mild cognitive impairment to Alzheimer's disease. *Neurobiol Aging* 2019;82:102-9.
62. Rodriguez-Ortiz CJ, Prieto GA, Martini AC, et al. miR-181a negatively modulates synaptic plasticity in hippocampal cultures and its inhibition rescues memory deficits in a mouse model of Alzheimer's disease. *Aging Cell* 2020;19:e13118.
63. Derkow K, Rössling R, Schipke C, et al. Distinct expression of the neurotoxic microRNA family let-7 in the cerebrospinal fluid of patients with Alzheimer's disease. *PLoS One* 2018;16:e0200602.
64. Liu Y, He X, Li Y, et al. Cerebrospinal fluid CD4+ T lymphocyte-derived miRNA-let-7b can enhance the diagnostic performance of Alzheimer's disease biomarkers. *Biochem Biophys Res Commun* 2018;495:1144-50.